Low temperature sensitivity of upconversion emission in Y_2O_3:Yb,Tm and Y_2O_3:Yb,Ho powders

V. Lojpur[1], M. Nikolic[2], M. Medic[2], L. Mancic[1], O. Milosevic[1], M.D. Dramicanin[2]

[1]Institute of Technical Sciences of SASA K.Mihailova 35/IV, Belgrade, Serbia

[2]Vinča Institute of Nuclear Science, University of Belgrade, P.O. Box 522, Belgrade, Serbia

Introduction

Phosphors are materials composed of a transparent host and an activator, typically a small quantity of a transition metal or rare earth ion. After absorbing a specific form of energy, these materials emit light in the ultraviolet (UV), visible (VIS) or infrared (IR) spectral regions. Rare earth (RE^{3+}) ion doped materials have been widely used as fluorescent and light-emitting diodes (LED), biological labels, lasers and components in a variety of display technologies. Because the absorption and emission properties of phosphors change with temperature, they could find applications in optical temperature sensing devices. Phosphor thermometry represents an optical technique for surface temperature measurements that is based on the time and temperature dependence of phosphorescence intensity. The fluorescent intensity ratio (FIR) is the foremost technique used to reduce the influence of measurement conditions and improve the sensitivity of the measurement. This simple, non-contact and precise method is applicable over a wide temperature range (from 10 K to 2000 K) and involves the comparison of intensities of two emission lines or areas in photoluminescent spectra. Herein, we discuss the structural and optical characterization of Y_2O_3:Yb^{3+},Ho^{3+} and Y_2O_3:Yb^{3+},Tm^{3+} powders synthesized using the spray pyrolysis method. We also examine their emission properties in the temperature range of 10 K to 300 K to explore for the first time the possibility of utilizing these materials in low temperature sensing applications.

Materials and methods

Yttrium oxide powders doped with either Yb^{3+},Tm^{3+} or Yb^{3+},Ho^{3+} were synthesized *via* spray pyrolysis. The precursor solutions were composed of $Y(NO_3)_3{\cdot}6H_2O$, $Yb(NO_3)_3{\cdot}5H_2O$, Tm_2O_3 and Ho_2O_3 in appropriate stoichiometric ratios for generating the following compositions: $Y_{1.89}Yb_{0.1}Tm_{0.02}O_3$ and $Y_{1.89}Yb_{0.1}Ho_{0.02}O_3$. The nitrate salts were dissolved in distilled water, whereas the oxides were dissolved in hot nitric acid. The resulting precursors (containing either Tm^{3+} or Ho^{3+}) were atomized at 1.7 MHz using an ultrasonic aerosol generator (Profi Sonic-Prizma, Serbia) and then injected into a heated quartz tube by air flow (1.6 dm^3/min). Aerosol decomposition was performed at 900 °C. The droplet/particle residence time in the reactor was 21 s. The resulting powders were collected at the end of a quartz tube and thermally treated at 1100 °C for 24 h.

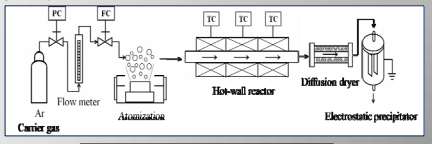

Fig. 1. Shematic description of spray pyrolysis

Results and discussion

The powders obtained via spray pyrolysis exhibit a cubic crystal structure, s.g. *Ia-3*, that corresponds to the $Y_{1.88}Yb_{0.12}O_3$ compound (PDF 87-2368). Fig. 2a provides the X-ray diffraction pattern of $Y_{1.89}Yb_{0.1}Ho_{0.02}O_3$ annealed at 1100 °C for 24 h. The typical morphology of particles synthesized using the spray pyrolysis method is shown in Fig. 2b. The resulting particles are spherical, sub-micronic in size and un-agglomerated. A closer inspection reveals that the particles are composed of smaller primary subunits, which give rise to a grainy surface appearance. Significant particle porosity is also observed.

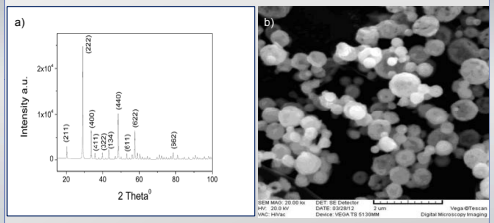

Fig. 2. X-ray diffraction pattern of Y_2O_3:Yb^{3+},Ho^{3+} powder annealed at 1100 °C for 24 h (a) and SEM image of same sample synthesized through spray pyrolysis (b)

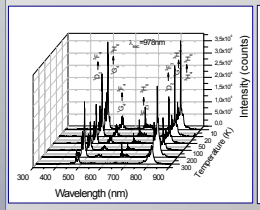

Fig. 3. Up-conversion spectra of Y_2O_3:Yb^{3+},Tm^{3+} in the VIS and IR regions

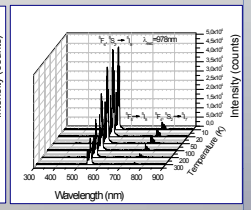

Fig. 4. Up-conversion spectra of Y_2O_3:Yb^{3+}, Ho^{3+} in the VIS and IR regions

The up-conversion emission spectra's of Y_2O_3:Yb^{3+},Tm^{3+} and Y_2O_3:Yb^{3+},Ho^{3+} were obtained using 978 nm laser excitation in the range of 10 K to 300 K. As shown in Fig. 3, three emission bands are observed for Tm^{3+}: a blue emission band (450-500 nm), a weak red emission band (650-680 nm) and a near infrared emission band (765-840 nm). The emission intensities of the red bands increase with decreasing temperature, whereas the blue and near infrared bands do not exhibit any obvious trends with varying temperature. As shown in Fig. 4, two emission peaks are observed for Ho^{3+}: a strong green emission peak centered at 550 nm and weak near infrared peak at 755 nm. Both emissions exhibit the same trends with increasing temperature, wherein the intensity significantly increases with decreasing temperature.

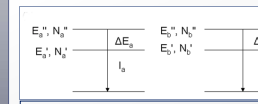

Fig. 5. A simplified diagram of transitions from the two excited states with a large energy difference

Thermalization process occurs between the Stark components of the excited levels, the emitted intensities are proportional to the population of each energy level, as shown in Fig. 5.

$$N_a'' = N_a' \exp(-\Delta E_a/kT), \quad N_b'' = N_b' \exp(-\Delta E_b/kT),$$

$$FIR = \frac{I_a}{I_b} = \frac{N_a''}{N_b''} = C\exp(-(\Delta E_a - \Delta E_b)/kT),$$

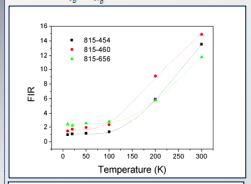

Fig.6. Intensity ratio of Y_2O_3:Yb^{3+},Tm^{3+} emission at 815 nm relative to emissions at 454 nm, 460 nm and 656 nm

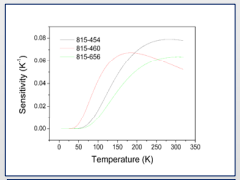

Fig.7. Temperature dependence sensitivity of FIRs in Y_2O_3:Yb^{3+},Tm^{3+} with emission at 815 nm relative to emissions at 454 nm, 460 nm and 656 nm

Table 1. Fitting results of the experimentally obtained FIRs for Y_2O_3:Yb^{3+},Tm^{3+}

FIR	C	ΔE_a - ΔE_b [cm^{-1}]	S_{max} [K^{-1}]	R_{adj}
I_{815}/I_{454}	82.76	394	0.078	0.9997
I_{815}/I_{460}	45.88	257	0.067	0.9959
I_{815}/I_{656}	71.85	425	0.064	0.9979

At temperatures of 270, 178 and 290 K, the sensitivity of Tm^{3+} exhibited maximum values of 0.078, 0.067 and 0.064 K^{-1} for the 815/454, 815/440 and 815/656 emissions ratios, respectively.

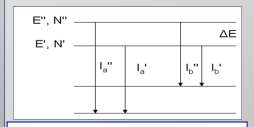

Fig. 8. A simplified diagram of transitions from the two excited states with a large energy difference

$$I_a = I_a'' + I_a' = N'' \omega_a g''(h\nu) + N' \omega_a' g'(h\nu),$$

$$I_b = I_b'' + I_b' = N'' \omega_b g''(h\nu) + N' \omega_b' g'(h\nu),$$

$$N'' = N' \exp(-(E'' - E'')/kT) = N' \exp(-\Delta E/kT),$$

$$FIR = \frac{I_a}{I_b} = \frac{1 + C_1 \exp(-\Delta E/kT)}{C_2 + C_3 \exp(-\Delta E/kT)},$$

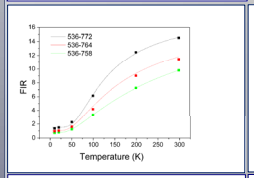

Fig. 9. Intensity ratio of Y_2O_3:Yb^{3+},Ho^{3+} emission at 536 nm relative to emissions at 772 nm, 764 nm and 758 nm

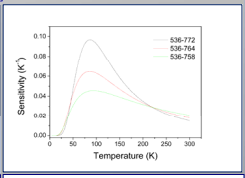

Fig.10. Temperature dependence sensitivity of FIRs in Y_2O_3:Yb^{3+},Ho^{3+} with emission at 536 nm relative to emissions at 772 nm, 764 nm and 758 nm

Table 2. Fitting results of the experimentally obtained FIRs for Y_2O_3:Yb^{3+},Ho^{3+}

FIR	C_1	C_2	C_3	ΔE [cm^{-1}]	S_{max} [K^{-1}]	R_{adj}
$I_{536.5}/I_{758}$	11.94	1	0.37	114	0.046	0.9999
$I_{536.5}/I_{764.8}$	25.55	1	0.46	131	0.065	0.9994
$I_{536.5}/I_{772.6}$	73.34	1	3.09	170	0.097	0.9980

At temperatures of 85, 84 and 90 K, the sensitivity of Ho^{3+} exhibited maximum values of 0.097, 0.065 and 0.046 K^{-1} for emissions at 536/772, 536/764 and 536/758.

Conclusion

Yttrium oxide powders doped with either Yb^{3+},Tm^{3+} or Yb^{3+},Ho^{3+} were synthesized *via* the spray pyrolysis method. Spherical, sub-micrometer, un-agglomerated porous particles, composed of smaller primary subunits, exhibit a significant temperature sensitivity of up-conversion emission. In the case of Y_2O_3:Yb^{3+},Tm^{3+}, the temperature dependence of the emission intensity ratios of excited states with a large energy difference is due to the thermalization between the Stark components in the excited states. In the case of Y_2O_3:Yb^{3+},Ho^{3+}, emissions occur from adjacent excited states to two lower states, so the temperature dependence of the emission intensity ratio is a consequence of the thermalization between adjacent excited states. The observed temperature sensitivity of both systems is significant enough for thermometry applications in the range of 10 to 300 K.

Literature

J. Brubach , T.Kissel , M.Frotscher , M.Euler , B.Albert , A.Dreizler, A survey of phosphors novel for thermometry, J. Lumin. 131 (2011) 559-564.

F. Wang, X. G. Liu, Upconversion Multicolor Fine-Tuning: Visible to Near-Infrared Emission from Lanthanide-Doped $NaYF_4$ Nanoparticles, J. Am. Chem. Soc. 130 (2008) 5642-5643.

H. Eilers, Effect of particle/grain size on the optical properties of Y_2O_3:Er,Yb, J. Alloys Compd. 474 (2009) 569-572.

F. Vetrone, J. C. Boyer, J. A. Capobianco, A. Speghini, M. Bettinelli, Significance of Yb^{3+} concentration on the upconversion mechanisms in codoped Y_2O_3:Er^{3+}, Yb^{3+} nanocrystals, J. Appl. Phys. 96 (2004) 661-667.

X. X. Luo, W.H. Cao, Upconversion luminescence of holmium and ytterbium co-doped yttrium oxysulfide phosphor, Mater. Lett. 61 (2007) 3696-3700.

S.A. Wade, S.F. Collins, G.W. Baxter, Fluorescence intensity ratio technique for optical fiber point temperature sensing, J. Appl Phys. 94 (2003) 4743-4757.

N. Ishiwada, T. Ueda, T. Yokomori, Characteristics of rare earth (RE = Eu, Tb, Tm)-doped Y2O3 phosphors for thermometry, J. Biol. Chem. Lumin. 26 (2011) 381-389.

P. Haro-González, S.F. León-Luis, S. González-Pérez, I.R. Martín, Analysis of Er^{3+} and Ho^{3+} codoped fluoroindate glasses as wide range temperature sensor, Mater. Res. Bull. 46 (2011) 1051–1054.

Acknowledgement

This research is financially supported by the Projects 45020 and 171022 of the Ministry of Science and Education of the Republic of Serbia.